

Formation and Collapse of False Vacuum Bubbles in Relativistic Heavy-Ion Collisions

Rajarshi Ray ^{*}, Soma Sanyal [†], and Ajit M. Srivastava [‡]
Institute of Physics, Sachivalaya Marg, Bhubaneswar 751005, India

Abstract

It is possible that under certain situations, in a relativistic heavy-ion collision, partons may expand out forming a shell like structure. We analyze the process of hadronization in such a picture for the case when the quark-hadron transition is of first order, and argue that the inside region of such a shell must correspond to a supercooled (to $T = 0$) deconfined vacuum. Hadrons from that region escape out, leaving a bubble of pure deconfined vacuum with large vacuum energy. This bubble undergoes relativistic collapse, with highly Lorentz contracted bubble walls, and may concentrate the entire energy into extremely small regions. Eventually different portions of bubble wall collide, with the energy being released in the form of particle production. Thermalization of this system can lead to very high temperatures. With a reasonably conservative set of parameters, at LHC, the temperature of the hot spot can reach as high as 3 GeV, and well above it with more optimistic parameters. Such a hot spot can leave signals like large P_T partons, dileptons, and enhanced production of heavy quarks. We also briefly discuss a speculative possibility where the electroweak symmetry may get restored in the highly dense region resulting from the decay of the bubble wall via the phenomenon of non-thermal symmetry restoration (which is usually employed in models of pre-heating after inflation). If that could happen then the possibility may arise of observing sphaleron induced baryon number violation in relativistic heavy-ion collisions.

PACS numbers: 25.75.-q, 12.38.Mh, 98.80.Cq

Typeset using REVTeX

*e-mail: rajarshi@iopb.res.in

†e-mail: sanyal@iopb.res.in

‡email: ajit@iopb.res.in

I. INTRODUCTION

There are strong reasons to believe that in ultra-relativistic collisions of heavy nuclei, a hot dense region of quark-gluon plasma (QGP) may get created. There is a wealth of data which strongly suggests that already at CERN SPS this transient QGP state may have been achieved [1]. With new data already coming out from RHIC at BNL [2], it may be only a matter of time that conclusive evidence of QGP detection would be obtained. Certainly, one expects that at LHC (in next few years) QGP will be produced routinely. There is no question that detection of this new phase of matter will be of utmost importance, not just for testing predictions of QCD, but also in providing us glimpses of how our universe may have looked like at few microseconds of age. It seems to be an appropriate stage that one starts looking beyond the detection of the QGP phase. Many interesting possibilities have been discussed in the literature about physical processes which may become observable once QGP is produced in laboratory. For example, one will have the opportunity of studying phase transitions in a relativistic field theory system under controlled laboratory situations. The richness of QCD phase diagram may become available for probing with quark-hadron transitions occurring in these experiments [3].

In this paper we propose a novel possibility of forming a pure false vacuum bubble in a relativistic heavy-ion collision, whose collapse and decay can lead to extremely hot, tiny regions, with temperatures well above the initial temperature of the QGP system. We assume that the confinement-deconfinement phase transition is of first order, and show that such a false vacuum bubble will form if the parton system (formed in the collision) expands out in a shell like structure, leaving behind the supercooled deconfined phase with large vacuum energy density. Eventually, as the partons hadronize and escape out, the interface, separating this false vacuum bubble from the confined phase outside, undergoes relativistic collapse. Due to absence of any plasma inside, the motion of this interface becomes ultra-relativistic, with highly Lorentz contracted interface thickness. Entire energy of the false vacuum bubble gets converted to the kinetic energy of the wall. Eventually different portions of bubble wall collide, converting the entire energy into particles. These particles may thermalize and lead to an extremely hot, very tiny region (apart from possible effects of quantum fluctuations of the bubble wall, as we discuss later). We find that even at RHIC energies, the temperature at these hot spots can be more than 1 GeV. For LHC the temperature can reach several GeVs. This will have important signals such as increased production of heavy quarks, anomalously large values of P_T of some hadrons (those coming from the hot spot) etc. Also, the net energy of the false vacuum bubble may be very large even at RHIC (~ 1 TeV), hence the possibility of Higgs and top quark production may also arise (depending on the decay products of the bubble wall).

At LHC energies, the net energy of this false vacuum bubble is very large which should lead to very dense parton system after the bubble wall decay. Due to initial very large density of partons at such a spot (forming a non-equilibrium system) we speculate on the possibility that electroweak symmetry may get restored there via the phenomenon of non-thermal symmetry restoration, as in the models of pre-heating after inflation [4]. If that could happen then it raises the possibility that sphaleron transitions may occur in these regions (depending on the size of such a region), which will lead to baryon number non-conservation. It is needless to say that any possibility of detection of electroweak baryon number violation

in laboratory experiments deserves attention, especially with its implications for the theories of baryogenesis in the early universe. We mention here that the possibility of baryon number violation in collider experiments has been discussed earlier, see, ref. [5] and references therein. However, the discussion in these works was about possibility of baryon number violation at high energies, and not due to electroweak symmetry restoration. It is fair to say that at this stage it is not clear whether it is possible to get baryon number violating interactions at high energies. However, baryon number violation in the electroweak symmetric phase is on rather strong foundations [6,7,8], and our reference is to this type of baryon number violation.

The paper is organized as follows. In section II, the basic physical picture of the model is discussed where it is argued how a shell enclosing deconfined vacuum may form in ultra-relativistic heavy-ion collisions. Section III discusses the properties of the shell, the surface energy, volume energy etc. Section IV discusses the evolution of this shell and its final ultra-relativistic collapse leading to high concentration of energy in a tiny region. In section V we discuss the issue of thermalization of the decay products of bubble wall. Section VI presents results for various ranges of parameters for LHC and RHIC energies, as well as for the possibility of non-thermal restoration of the electroweak symmetry. Discussion of results and the conclusion is presented in section VII.

II. PHYSICAL PICTURE OF THE MODEL

The main aspect of our model is based on the observation [9] that under certain situations, the expanding parton system may form a shell like structure. This type of picture emerges under a variety of conditions. For example, in a hydrodynamical expansion, the rarefaction wave reaching center gives rise to a shell like structure [9]. (We mention, that shell like structure with a *maximum* of density at center has also been discussed in the literature [10].) It has been shown that shell structure will arise generically in an expanding parton system when partons are ultra-relativistic and particle collisions are not dominant [9]. This happens for the simple reason that with all partons having velocity $\simeq c$, the partons pile up in a shell of radius $\simeq c \times t$, with the thickness of the shell being of the order of the size of the initial region. Indeed, the original so called *baked Alaska* model for the disoriented chiral condensates, proposed by Bjorken et al. [11] utilizes a shell like picture for the expanding parton systems (see also, ref. [12] where a similar picture has been discussed). Our model is based on this generic shell structure of the parton system.

However, there is one important difference between our model and other discussions in the literature where a shell like structure of partons has been discussed. In refs. [11,12], the discussion was in the context of a second order chiral phase transition where the larger potential energy of the inside region slowly decreases as the chiral field relaxes towards the true vacuum. In contrast, our model is based on a first order confinement-deconfinement phase transition, where the vacuum energy of the inside region can only decrease by collapse of the interface, or via nucleation of true vacuum bubbles in this region, which we will argue to be very suppressed. Though we have presented the discussion in terms of a first order deconfinement-confinement transition, our entire discussion will also be valid for a first order chiral phase transition. Basic energy scales of these two transitions being roughly of same

order, even quantitative aspects of the discussion will not change much. In discussions of [9] it is argued that the hadronization in the shell will proceed from the inner boundary of the shell, as well as the outer boundary of the shell. This assumes that the *empty* region inside the shell will be in the confined vacuum. We argue below that there is no reason to expect that. Rather, one expects that the shell of partons will enclose a region of deconfined vacuum.

Let us start with the initial stage of central collision of two nuclei. For very early stages after the collision, the region between the two receding nuclei will be populated by a dense system of partons, with a temperature which is expected to be well above the critical temperature T_c of deconfinement-confinement phase transition (at RHIC and LHC). (We will consistently refer to the phase transition as the deconfinement-confinement (D-C) phase transition rather than using the conventional terminology of quark-hadron transition. This is because we will utilize the difference between the vacua of the two phases of QCD, irrespective of the fact whether these vacua are populated by quark-gluon, or hadron degrees of freedom.) Subsequently, plasma will expand longitudinally for early times (for $\tau < R_A$, where τ is the proper time and R_A is the radius of the nucleus), and will undergo three-dimensional expansion for larger times. For heavy nuclei with large A , and for center of mass energies at RHIC and LHC, it is expected that the plasma will undergo deconfinement-confinement phase transition during this three dimensional expansion stage, and later the expanding hadronic system will freezeout. In various models of freezeout, it is argued that the freezeout happens soon after the D-C phase transition and that this stage is achieved at proper time hypersurface which is close to the hypersurface when three-dimensional expansion commences [13] (see, also ref. [14]).

The expected value of central energy density ϵ_i at the initial stage (hence the initial temperature T_i), increases with A and with \sqrt{s} . An estimate of the dependence of ϵ_i on A and \sqrt{s} can be obtained from the scaling relations proposed in ref. [15] (see also, ref. [16]),

$$\epsilon_i = 0.103A^{0.504}(\sqrt{s})^{0.786} \text{ GeVfm}^{-3}, \quad (1)$$

where \sqrt{s} is in GeV. These scaling exponents reproduce the expected values of initial energy density for SPS, RHIC and LHC. Thus, for LHC, with $A = 208$ and $\sqrt{s} = 5.5$ TeV (we will use \sqrt{s} to refer to \sqrt{s} per nucleon), we find $\epsilon_i \simeq 1.3$ TeV/fm³ which is within the range of other estimates [17].

We note that dependence on A is somewhat weaker than the dependence on \sqrt{s} . Thus, if one decreases value of A and increases \sqrt{s} suitably, one can still get large ϵ_i (suitable for having a QGP state initially at temperatures well above T_c). However, with lower value of A , R_A will be smaller ($R_A \simeq 1.1A^{1/3}$), implying that the three-dimensional expansion will commence at earlier values of proper time. This will have two effects. Temperature will decrease faster ($T \sim \tau^{-1}$ for three-dimensional expansion while $T \sim \tau^{-1/3}$ for longitudinal expansion [18]). More importantly, with rapidly expanding system, thermodynamic equilibrium will be maintained for a shorter duration of proper time, implying that freezeout will happen earlier. In principle, there is no reason why freezeout cannot precede the D-C phase transition. In such a situation, initial thermalized QGP system expands longitudinally for a short time, then undergoes three dimensional expansion. Due to rapid 3-dimensional expansion, the system falls out of equilibrium and keeps expanding as a parton system in a

non-equilibrium state (still with high density of partons so that no hadronization takes place yet). Eventually the parton system will be dilute enough to enter into the non-perturbative regime, and will undergo hadronization. This process of hadronization will be in a non-equilibrium state, where a parton system out of equilibrium converts to a hadron system (again, out of equilibrium). Possibility of freezeout preceding hadronization has also been discussed previously in ref. [19]. A quantitative discussion of the limiting values of \sqrt{s} , and that of A below which freezeout may precede hadronization, can only be given using elaborate numerical computations (such as those in ref. [13]).

In such a picture of expansion of parton system, it is possible to have the central region (in the shell) depleted of partons while the partons get accumulated in the shell. Thus, central region *does not cool* to become zero temperature, zero density QCD matter, as would happen if the system was always in thermal equilibrium (and that would then require that the interior of the shell be in the confined vacuum, as assumed in [9]). Rather, in the above picture, the interior of the shell is depleted of partons because of rapid expansion of the parton system. As thermal equilibrium is not maintained, parton collision rate lags behind the expansion rate. As mentioned above, in such a situation the analysis of refs. [9] suggests that partons, due to their relativistic velocities, pile up in a shell of radius $R \simeq c \times t$ where t is the time in the center of mass frame of the collision. The thickness of the shell Δr will be expected to be of the order of the size of the region when thermal equilibrium is first broken such that parton system undergoes almost free expansion after that.

We mention here that it is conceivable that the initial parton system never thermalizes (for example for very small A), but nevertheless, deconfinement phase is achieved. This possibility can originate from the discussions of non-thermal symmetry restoration in the context of inflation in the early universe [4]. In these works it is shown that rapid particle production due to parametric resonance can lead to modification of the effective potential, even without any notion of thermal equilibrium. Under certain situations the symmetry restoration can be achieved even when thermal symmetry restoration is not expected. The early stages in nucleus-nucleus collisions resemble the stage of parametric resonance at least in the sense of rapid particle production. It is then possible that in this case also deconfinement phase is achieved with parton system always remaining out of equilibrium. This system will then undergo expansion forming a shell structure [9] before hadronizing eventually. (Later, in Sec.VI, we will discuss whether a similar picture can also emerge for the decay products of bubble wall, leading to non-thermal restoration of the electroweak symmetry even when the system remains in a non-equilibrium state.)

Thus, we assume that the expanding parton system forms a shell, with the interior of the shell being in the deconfined vacuum. At the outer boundary of the shell there must be an interface separating the deconfining vacuum in the interior from the confining vacuum in the outer region [20]. (We are assuming the D-C transition to be of first order, with a barrier separating the metastable deconfined vacuum from the true confining vacuum, even at temperatures approaching zero. We will discuss this issue in detail below.) Partons will be piled up inside the shell, within a thickness Δr of the interface. The center of the shell interior thus represents a supercooled (to $T = 0$) region trapped in the metastable deconfining vacuum.

It is somewhat uncommon to talk about zero temperature deconfining phase of QCD. Normally one associates deconfinement phase with the quark-gluon plasma at temperatures

above T_c . However, it is important to distinguish the vacuum of a theory from the particle excitations about that vacuum. Confining phase and the deconfining phase of QCD should be taken to correspond to the two different vacua of some effective theory of QCD, with the deconfining vacuum being metastable at zero temperature. The two vacua may be characterized by an order parameter, such as the expectation value of the Polyakov line [21]. That means that certain type of gauge field background leads to one vacuum, while a different gauge field background gives the different vacuum. These two vacua are thus defined irrespective of the presence or absence of quarks and gluons, or hadrons, as particle degrees of freedom (except as test particles in order to define confinement). It then makes sense to talk about deconfining vacuum without any quark or gluon being present as particle degrees of freedom, though this vacuum will be metastable. (For example, if the chiral phase transition is of first order, with a chirally symmetric vacuum even at $T = 0$, then it will make perfect sense to talk about a supercooled chirally symmetric phase with $T = 0$.)

The type of picture we are taking in our model, with the shell interior depleted of quarks and gluons but still trapped in the metastable deconfining vacuum, is very similar to what happens in the inflationary theories of the universe [22]. For example, in the old inflation, the scalar field ϕ gets trapped in the false vacuum and supercools as the universe undergoes exponential expansion due to non-zero potential energy of ϕ . Initially the universe is filled with scalar particles (as well as other particles) in thermal equilibrium corresponding to a temperature above the transition temperature. However, due to exponential expansion, initially the system cools maintaining equilibrium, but then falls out of equilibrium with all particles undergoing depletion due to exponential expansion of the universe. Eventually the particles are completely diluted away, while the universe still remains in the metastable vacuum. This is precisely the same picture as we are using in our model. The only thing required for such a picture is that QCD admit a metastable vacuum even at zero temperature. The exponential expansion of the universe is replaced by rapid outward expansion of partons in our case. Possibility of supercooling and a brief inflationary phase at quark-hadron transition in the universe has also been discussed in the literature [23].

III. PHYSICAL PROPERTIES OF THE SHELL

It is perfectly sensible to believe that QCD admits a metastable vacuum even at zero temperature. The entire physics of Bag model is within this type of framework. Inside of the bag is in the deconfining vacuum which is metastable with higher potential energy (the bag constant). The region outside the bag is in the confining vacuum with zero potential energy, with a wall separating the two regions. This is entirely consistent with the picture of a first order deconfinement-confinement phase transition at finite temperature where one usually writes down a finite temperature effective potential as a function of an appropriate order parameter. The expectation value of the Polyakov line $\langle L \rangle$ has been used to describe the physics of this phase transition at finite temperature [21,24], where $\langle L \rangle$ is given by,

$$\langle L \rangle = \frac{1}{N_c} \langle \text{tr} P e^{i \int_0^\beta A_0 d\tau} \rangle, \quad (2)$$

where N_c is the number of colors, $\beta = 1/T$, P denotes path ordering, and A_0 is the time

component of the vector potential. $\langle L \rangle$ vanishes in the confining phase, while it is non-zero in the deconfining phase, breaking the $Z(3)$ symmetry spontaneously [21,24].

On the other hand, at $T = 0$, the physics of bag model can be captured by postulating a color dielectric field χ with the following form of the effective potential for χ [25,26],

$$V(\chi) = \frac{m_{gb}^2}{2}\chi^2\left[1 - 2\left(1 - \frac{2}{\alpha}\right)\frac{\chi}{\sigma_v} + \left(1 - \frac{3}{\alpha}\right)\frac{\chi^2}{\sigma_v^2}\right]. \quad (3)$$

with corresponding Lagrangian density being $L = \frac{1}{2}(\partial_\mu\chi)^2 - V(\chi)$. Here, $\sigma_v = \sqrt{2\alpha B/m_{gb}^2}$, m_{gb} is the glueball mass and B is the bag constant. We take $\alpha = 24$, $B^{1/4} = 122.3$ MeV, and $m_{gb} = 978.6$ MeV. These are the parameter values used in ref. [25], and we use these as a sample. The relevance of these parameters for us is in determining the values of surface tension σ and false vacuum energy density ρ of the deconfining bubble. We will present results for a wide range of σ and ρ .

The plot of $V(\chi)$ is shown in Fig.1. $\chi = 0$ in the confining region outside the bag, while it has a non-zero value in the deconfining region inside the bag. χ thus has the same physical behavior as $\langle L \rangle$, the expectation value of the Polyakov line L . It would seem rather superfluous to have two entirely different characterizations of same physical phenomenon, i.e. two different phases of the same system, separated by an interface. One would like to think of the color dielectric field χ as capturing the physics of $\langle L \rangle$. With this identification, one has a single, unifying picture where the effective potential for a strongly interacting system is always of the form given in Eq.(3), with χ being interpreted as either the color dielectric field of the bag model, or the expectation value of the Polyakov line L (neglecting the symmetry aspects of the order parameter). At finite temperature, the coefficients in $V(\chi)$ will become temperature dependent which will change the values of surface tension of the interface, latent heat etc. compared to the values obtained from the parameter values given above. The important thing is that the barrier between the deconfining vacuum and the confining vacuum must survive even at $T = 0$ if the physics of the bag model has to be preserved. We mention that the forms of effective potential such as the one used in ref. [27] do not capture this physics of deconfinement-confinement phase transition. For example, in ref. [27], an effective potential has been used with a $T\phi^3$ term (with ϕ being the order parameter for D-C phase transition) to model the first order nature of the transition. Thus in this model, barrier between the deconfining vacuum and the confining vacuum disappears below certain temperature, which is not in the spirit of the physics of bag model. For the same reason we do not use the parameterization used in ref. [24] as that model also is appropriate for describing physics near and above T_c .

The final picture of our model can now be presented. We start with the initial time τ_i , with dense partons filling the collision region. This parton region will correspond to the region between the two nuclei, receding after overlap, with transverse radius of the region being equal to R_A , the nuclear radius. Much of the collision energy will be carried by partons in the fragmentation region. We are interested in the total energy available to the expanding parton system in the central region, which will eventually lead to the formation of the false vacuum bubble. For this, we take the total energy E_{tot} to be,

$$E_{tot} = \epsilon_i\pi R_A^2\Delta z_i, \quad (4)$$

where ϵ_i is the initial energy density expected in the collision (as given in Eq.(1)). $R_A \simeq 1.1A^{1/3}$ fm, and Δz_i is the initial thickness of the central region. For central region near $z = 0$, Δz_i corresponding to a rapidity interval ΔY at the initial time τ_i can be taken as $\Delta z_i = \tau_i \Delta Y$ (see, ref. [16]). Estimates for τ_i , initial QGP formation time, vary from $\tau \sim 0.15$ fm (for LHC) to $\tau \sim 0.22$ fm for RHIC. In view of various uncertainties [15,16,17] in the estimates of ϵ_i , and τ_i , (as well as in determining the relation between the plasma formation time τ_i and the initial longitudinal extent of the plasma), we will present results for several values of Δz_i . We will take $\Delta z_i = 0.15$ fm for LHC, and equal to 0.22 fm for RHIC, and an optimistic value $\Delta z_i = 1$ fm for both LHC and RHIC which will correspond to a large value of E_{tot} . It is important to mention that our results only depend on the value of E_{tot} . Thus, large value of E_{tot} may arise from uncertainties in ϵ_i , or Δz_i . For Pb-Pb collision at LHC with $\sqrt{s} = 5.5$ TeV, expected initial energy density in the central region is about $1.3 \text{ TeV}/fm^3$. This gives $E_{tot} \simeq 25$, and 175 TeV corresponding to $\Delta z_i = 0.15$, and 1 fm respectively. For Au-Au collision at RHIC with $\sqrt{s} = 200$ GeV, the energy is much smaller and we find $E_{tot} \simeq 3$, and 10 TeV for $\Delta z_i = 0.22$, and 1 fm respectively.

This parton system then expands and cools (for non-equilibrium expansion, we say that the energy density of parton system decreases as temperature may not be defined). Important thing is that at the initial time τ_i , the parton system must be in the deconfining phase (either due to temperature $> T_c$, or due to non-thermal transition with extremely high energy density of partons). The region outside the initial parton system being in the confining phase, there must be an interface separating the two regions. Fig.2a shows such a situation.

Initial expansion will be longitudinal for proper times $\tau < R_A$, and will become three-dimensional expansion for larger times. It is expected that energy density (or the temperature) still remains sufficiently high so that by the time expansion becomes three-dimensional, the parton system still remains in the deconfining phase. Fig. 2b denotes such a stage of the central parton system at $\tau \simeq R_A$. (We mention here that it is not crucial for our model whether the fragmentation region is inside this region shown in Fig.2b, or falls outside it.) For subsequent expansion, we assume (as explained in detail above) that a shell structure starts developing. For times much larger than R_A , one expects an almost complete depletion of partons in the central region [9], with all partons piled up near the shell boundary. Fig. 2c denotes this intermediate stage. (We can take the proper time τ as measured in a frame at rest at some average point in the middle of the shell. Velocity there will not be very close to c , so τ will not be much different from the time t in the center of mass frame. In any case, the 3-dimensional expansion is not expected to be ultra-relativistic, so at this stage, one can use τ and lab time t interchangeably. We also neglect any Lorentz contraction in the thickness of the parton shell.) The stage shown in Fig.2c is the non-trivial part of our model. Here, the entire region inside the sphere of radius $\simeq ct$ is taken to be in the deconfining vacuum. There is then the interface at the boundary. The partons accumulate near the boundary of the shell from inside. The thickness of this region containing the partons will be expected to be of order of about $2 \times R_A$ as that is the total extent of the region at the time at which three dimensional expansion begins.

The region with $r < ct - 2R_A$ has no partons, but is still in the deconfining vacuum. This somewhat unconventional picture can be further justified as follows. Starting from a stage as shown in Fig.2b, where the entire interior region was in the deconfining vacuum,

one reaches the stage shown in Fig.2c by parton expansion. The inner region (devoid of partons) can turn into the confining vacuum only if there is nucleation of bubbles of confining vacuum in that region, which upon coalescing will convert the inner region into the confining vacuum. This could happen if the inner region cooled to $T = 0$ (with zero parton density, assuming zero baryon number in the central region) maintaining thermal equilibrium. However, thermal nucleation of bubbles could not happen since we are assuming that freezeout occurred before the hadronization transition (or, due to large time scales of bubble nucleation [28]). Even if the system did not go through finite temperature bubble nucleation when temperature decreased below T_c , the inside region can still be in the confining vacuum if quantum nucleation of confining vacuum bubbles (at $T = 0$) could happen. As we will discuss below, the action S_0 of such a bubble is about 100 in natural units. The probability of nucleation of such a bubble is proportional to e^{-S_0} , and hence is completely negligible for the relevant time scales, allowing for reasonable dimensional estimates for the pre-factor for the nucleation probability. (As in our model a significant barrier separating the two vacua remains even at $T = 0$, there is no possibility of the phase transition occurring via spinodal decomposition.) Thus, we conclude that the inner region of the shell must correspond to $T = 0$ supercooled deconfining vacuum.

Eventually, as parton shell keeps expanding, its energy density falls below a critical value so that hadronization must take place. Partons will then form hadrons as they leave the spherical region bounded by the interface. This is the stage when the interface will stop moving outward, and will start shrinking. As the interface passes through the parton system, it converts partons into hadrons, as shown in Fig.2d. (Alternatively, hadronization may happen at various places in the parton shell. This will also amount to an effective shrinking of the interface.) The motion of the interface will be dissipative at this stage due to its interaction with partons. Typical velocity of the interface, therefore, will be less than the speed of sound [29,27,28]. However, as all (or most) of the partons hadronize, the interface will continue to move inward due to negative pressure of the metastable vacuum. Now there are no partons to impede the motion of the interface. What one is left with is a spherical bubble of pure false vacuum. To obtain the profile of the wall of this *false vacuum* bubble, we first obtain the profile of the *true vacuum* bubble as follows. Given $V(\chi)$ in Eq.(3), one can obtain the instanton solution for the tunneling through the barrier from $\chi \neq 0$ metastable vacuum to the $\chi = 0$ true vacuum. This is given by the solution of the following equation [30],

$$\frac{d^2\chi}{dr^2} + \frac{\kappa}{r} \frac{d\chi}{dr} - V'(\chi) = 0, \quad (5)$$

where $V(\chi)$ is the effective potential in Eq.(3) and r is the radial coordinate in the Euclidean space. In the Minkowski space initial profile for this true vacuum bubble is obtained by putting $t = 0$ in the solution of the above equation. Parameter $\kappa = 3$ for quantum nucleation of bubble (at $T = 0$), while $\kappa = 2$ for thermal nucleation of bubble at finite temperature. Initially the parton region had large temperature, so the profile of the interface at that stage would be given by the finite temperature bubble (i.e. $\kappa = 2$). This will be true up to the stage shown in Fig.2b. After freezeout, or once the partons leave the shell in the form of hadrons as in Fig.2e, the profile of the interface will be given by $T = 0$ bubble, that is $\kappa = 3$ case. We have solved Eq.(5) using a fourth order Runge Kutta algorithm for the

effective potential as given in Eq.(3). The numerical technique is the same as used earlier for standard false vacuum decay [31] with the obvious difference that now the false vacuum occurs at non-zero value of χ while the true vacuum occurs at $\chi = 0$. Thus the search for the bounce solution has to be done differently in the present case. In Fig.3a we have shown the solution of the $T = 0$ quantum bubble of true vacuum. The radius of this bubble is about 5 fm. (The finite temperature bubble has a smaller radius $\simeq 3.8$ fm.) We have calculated the action for the true vacuum bubble shown in Fig.3a and we find it to be about 100 in natural units. As mentioned above, this large value of the action suppresses the nucleation of true vacuum bubbles in the the central deconfined ($T = 0$) region, so that this region converts to the confining vacuum only via collapse of the spherical interface shown in Fig.2e.

Fig.3a shows the bubble of confining vacuum embedded in the deconfining vacuum (as obtained by the instanton solution of Eq.(5)). However, the experimental situation we have discussed above is exactly the reverse. As shown in Fig.2e, we have a large bubble of deconfining vacuum which is embedded in the confining vacuum. Such a bubble cannot be obtained as a classical solution of Eq.(5). The situation shown in Fig.2 arises because of changing temperature, and is similar to the false vacuum bubble formation due to coalescence of true vacuum bubbles as discussed in the context of quark-hadron transition in the early universe [32]. Main difference between our case and the case discussed in ref. [32] (see, also ref. [28]) is that there the motion of bubble wall remains dissipative due to presence of QGP in the interior of the bubble. In contrast, in our case, the special geometry of collision gives the shell like structure which leads to a pure false vacuum bubble with no QGP inside. The motion of the interface, therefore, will not be dissipative. Fig.3b shows this false vacuum bubble which is simply obtained by inverting the profile of the bubble as given in Fig.3a. This is a somewhat approximate way of generating the appropriate bubble profile. However, our interest is only in the values of surface tension σ of the interface and the false vacuum energy density ρ . (Note that ρ is the same as the bag constant B . We use a different notation for it due to the method by which we calculate it by generating the confining vacuum bubble and then inverting it.) We will present results for a range of values of these parameters, with the profile given in Fig.3b corresponding to one set of these values. Note that the radius of this deconfining vacuum bubble (Fig.3b) is not obtained from equation of motion. In contrast, radius of the confining vacuum bubble of Fig.3a was fixed by the solution of Eq.(5). Inverted profile in Fig.3b is generated only to estimate the values of σ and ρ corresponding to parameter values in Eq.(3). Its radius will be determined by the physics of the problem, such as total energy of collision, as we discuss below. In the same way, the radius of the false vacuum bubble in ref. [32] is determined by separation between the nucleation sites of the hadronic bubbles, and the manner in which they coalesce.

To obtain values of surface tension σ and the false vacuum energy density ρ of the deconfining vacuum bubble, we obtain total energy E of the false vacuum bubble by numerically integrating the energy density, $\frac{1}{2}(\nabla\chi)^2 + V(\chi)$, for the bubble profile in Fig.3b. Bubble energies are obtained in this manner for two different values of bubble radius. σ and ρ are then determined by using the following equation for the two values of bubble energy and radius,

$$E = 4\pi r^2 \sigma + \frac{4\pi}{3} r^3 \rho. \quad (6)$$

The values of σ and ρ obtained by using this equation for two values of bubble radius are tested for other bubble radii and it is found that bubble energies are accurately reproduced. For the parameters used for Eq.(3) in ref. [25], we find $\sigma = 64.8\text{MeV}/\text{fm}^3$ and $\rho = 27.8\text{MeV}/\text{fm}^3 (\simeq (122\text{MeV})^4)$. Note that this value of ρ is the same as the bag constant B in Eq.(3) as it should be. This gives us confidence that this procedure of inverting profile of confining vacuum bubble to get the profile of the deconfining vacuum bubble is reasonably accurate. For comparison, we repeated this procedure for the finite temperature bubble, i.e. solution of Eq.(5) with $\kappa = 2$, (pretending that the effective potential in Eq.(3) corresponds to the finite temperature case). As we mentioned, resulting bubble radius of the confining vacuum bubble (similar to the $T = 0$ bubble in Fig.3a) is about 3.8 fm. We find that the inverted bubble (deconfining vacuum bubble, as in Fig.3b) has $\sigma = 64.4 \text{ MeV}/\text{fm}^2$ and $\rho = 27.8 \text{ MeV}/\text{fm}^3$. These values are essentially the same as in the case of $T = 0$ bubble. Since the only thing we need from the above calculations is the values of these parameters, it is immaterial whether we think of the interface as corresponding to the finite temperature bubble or to $T = 0$ bubble.

IV. EXPANSION AND SUBSEQUENT ULTRA-RELATIVISTIC COLLAPSE OF THE SHELL

We need to make one further specification about the expansion of the parton system. If the expansion is adiabatic, then total entropy will be conserved. In that situation, total energy will decrease due to the work done by the pressure of the plasma. This description is appropriate when expansion happens maintaining equilibrium, as in the hydrodynamical models of parton expansion. In the situation of free expansion, or if there are dissipative effects present, then expansion could be energy conserving [33]. We have argued above that shell picture is more reasonable in the case when parton system freezes out early. Thus energy conserving expansion may be more appropriate for our model. We consider this case first. We will also briefly discuss results for the adiabatic expansion, and we will see that the temperatures of the hot spot are much smaller for that case. (Note that the only thing relevant to us about the parton expansion is the development of a shell structure with central region devoid of partons, but still in the deconfined vacuum. We have argued that this seems natural when partons freezeout early. However, all of our arguments are valid if this picture can be justified even by taking partons to be in equilibrium, through the stages in Fig.2a-2d.) Assuming the energy to be conserved, the energy density of the partons in the shell, $\epsilon(r)$, at any stage shown in Fig.2c, is determined by,

$$4\pi r^2 \sigma + \frac{4\pi}{3}(r^3 - (r - \Delta r)^3)\epsilon(r) + \frac{4\pi}{3}r^3 \rho = E_{tot}, \quad (7)$$

where E_{tot} is given in Eq.(4). Here $\epsilon(r)$ denotes the parton energy density in the shell of thickness $\Delta r \simeq 2R_A$. The shell will expand to a largest size r_{max} at which stage parton system will hadronize. We determine r_{max} by taking $\epsilon(r) = \epsilon_c$, the critical value of energy density of partons below which hadronization is expected to take place. We take $\epsilon_c \simeq \frac{\pi^2 37}{30} T_c^4$, where T_c is the critical temperature for the quark-hadron transition. ϵ_c is not to be taken necessarily as the energy density of plasma in equilibrium (with temperature = T_c), as we

have argued that the partons may be in a non-equilibrium state. We take ϵ_c as giving the scale below which partons should convert to hadrons. The value of T_c is related to the bag constant (for an equilibrium transition) using Gibbs criterion of equal pressure at transition temperature, $T_c = (B/(g_q - g_h))^{1/4}$. Here, $g_q = 37\pi^2/90$ and $g_h = 3\pi^2/90$, corresponding to 2 massless quark flavors and 8 gluons in the QGP phase, and 3 pions in the hadronic phase. Again, the value of B appropriate at the scale given by T_c may be different from the value of B at $T = 0$. For simplicity, we ignore any scale dependence of B and use the same value of B which equals the false vacuum energy density ρ , as also determining T_c via above relation. Therefore, we present results for a large range of values of B , not limiting to only those values which correspond to realistic values of T_c .

r_{max} gives the largest radius of the shell, with interface being at the outer boundary (i.e. at $r = r_{max}$) initially. As this is the stage when hadrons start forming, interface starts moving inwards. Initial motion of the interface is highly dissipative [29,27], as long as it traverses the region which is filled with the partons, i.e. a thickness of $\Delta r \simeq 2R_A$. This stage is shown in Fig.2d. Once the interface has shrunk below this parton filled region, it is free to undergo unimpeded, relativistic collapse. The region bounded by this interface at a later stage (shown in Fig.2e) represents a pure false vacuum bubble with no partons inside. The initial radius of this pure false vacuum bubble, r_f will be approximately given by,

$$r_f \simeq r_{max} - R_A, \quad (8)$$

where r_{max} is determined by solving Eq.(7) with $\epsilon(r) = \epsilon_c$. In writing this expression for r_f , we have taken that when $\epsilon(r) = \epsilon_c$ is achieved during the shell expansion, the interface starts collapsing with almost speed of light, as the parton shell keeps expanding relativistically. However, due to dissipative motion of the wall through the parton system, velocity of the wall will be typically much smaller than the speed of light [29]. If one takes the wall to be almost static, as compared to the outward velocity of the shell, then one will expect r_f to be almost equal to r_{max} . Thus, the value of r_f as given above is an underestimate. Resulting total energy of the false vacuum bubble, and hence the final temperature of the hot spot will also be somewhat underestimated in using the above equation. This should hopefully compensate, to some degree, the effects of assuming all partons to be ultra-relativistic, (e.g., if the parton distribution extends beyond the assumed shell thickness of $2r_{max}$, it will reduce the value of r_f).

Total energy E_f of this pure false vacuum bubble is,

$$E_f = 4\pi r_f^2 \sigma + \frac{4\pi}{3} r_f^3 \rho. \quad (9)$$

Further evolution of this false vacuum bubble is well understood. It will undergo relativistic collapse. Due to surface tension, bubble will become more spherical as it collapses. This is important as there are various factors because of which the initial shape of the bubble wall may not be spherical. First, the collision geometry itself will not be expected to give rise to completely spherical structure. Secondly, the interface motion through the parton shell itself may not be very isotropic. However, during the free collapse of the interface, the shape should become more spherical due to surface tension. Any remaining asphericity will ultimately affect the final radius to which the bubble can collapse before the bubble walls

decay via collision. For simplicity, we will assume that the interface collapses maintaining spherical symmetry. During bubble collapse, the potential energy of the false vacuum simply gets converted into the kinetic energy of the collapsing interface [30]. This is where our model crucially differs from the collapsing QGP bubbles previously discussed in the context of quark-hadron transition [32,28]. There, interface always moves through a QGP system filling the interior of the bubble, which impedes the motion of the interface. The false vacuum energy there gets converted to the heat which raises the temperature of the plasma [32,28]. In contrast, there are no partons in the interior of the deconfining vacuum bubble in our model. The entire false vacuum energy thus converts to the kinetic energy of the interface. The collapsing interface quickly becomes ultra-relativistic, with extremely large Lorentz contraction factor, as indicated by thinner interface in Fig.2e.

At any stage during the collapse of the shell, the value of the Lorentz γ factor primarily depends on the initial radius r_f of the shell, and the value of ρ (i.e. B). To give an idea of how rapidly the bubble wall Lorentz contracts, we give values of γ at the stage when the bubble has collapsed to a radius of 1 fm. For Pb-Pb collision with $\sqrt{s} = 5.5$ TeV, and with $\Delta z_i = 1$ fm, we find that r_f varies from 20 to 90 fm as $B^{1/4}$ is reduced from 240 MeV to 120 MeV (as we will see below). Value of γ , when bubble has collapsed to a radius of 1 fm, ranges from 3×10^4 to 8×10^4 . For same parameters, but with $\Delta z_i = 0.15$ fm, γ ranges from 2000 to 7000. At RHIC energy, with $\sqrt{s} = 200$ GeV for Au-Au collision (with $\Delta z_i = 1$ fm), r_f ranges from 5 fm to 35 fm as $B^{1/4}$ is reduced from 250 MeV to 100 MeV. Resulting γ factor (again, when bubble has collapsed to 1 fm radius) ranges from about 500 to 4000. For this case, by the stage when bubbles radius has decreased by another order of magnitude, i.e. to a value of 0.1 fm, γ ranges from about 5×10^4 to 3×10^5 .

The thickness of the interface initially (i.e. at stages shown in Fig.2a-2d), is about 1 fm. We see that by the time bubble collapses to a radius of about 1 fm, the thickness of the interface is much smaller, about 10^{-3} fm to 10^{-5} fm. Interface thickness reduces to about 10^{-5} fm to 10^{-7} fm by the time the bubble collapses to a radius of 0.1 fm. Again, it is unconventional to talk about such large length contraction factors in the context of heavy-ion collisions. We know that due to virtual partons at small x (the so called *wee partons*), nucleus thickness does not Lorentz contract below about 1 fm even at ultra-high energies [34] (see, also, ref. [35]). However, this limiting Lorentz contraction arises due to virtual particle production in the color field of the partons. In our case, by the time the interface contracts below the partonic shell, there will be no such virtual partons inside the bubble. Thus, there is no compelling reason to believe that the Lorentz contraction of the interface of this pure false vacuum bubble should be limited by the typical QCD scale of 1 fm. Basically, the radial profile of the interface represents the kink solution (Eq.(5)) which can be Lorentz boosted to any velocity in the absence of interactions with partons. Even with quantum fluctuations on the background of this ultra-relativistic bubble wall, there is no reason to expect that these fluctuations will put a stop to the highly Lorentz boosted bubble wall. Though some of the wall energy may get dissipated due to these effects, bubble collapse may still continue to sizes much smaller than 1 fm as long as walls remain ultra-relativistic.

This extreme Lorentz contraction of the bubble wall has following important consequence. Normally, the process of the collapse of a bubble wall will stop when its radius is of the order of the thickness of the wall. (See, for example, the numerical study of collapsing domain walls in ref. [36]). Though, for ultra-relativistic collapse numerical errors can build up and one

needs more sophisticated numerical techniques, see ref. [37].) Without significant Lorentz contraction, we would expect the bubble collapse to halt at the stage when bubble radius is of the order of 1 fm, as in the standard treatments of collapse of QGP bubbles in a quark-hadron transition [32]. Then bubble walls (of different bubble portions) will collide and the energy of walls will be released in the form of particle production. However, in our case the bubble wall undergoes large Lorentz contraction even when bubble radius is about 1 fm (in the center of mass frame). As compared to the wall thickness, bubble radius is about 10^3 to 10^5 times larger at this stage. Thus, there is no reason to expect that bubble collapse will halt at this stage. In fact it is easy to see (using the fact that as bubble collapses, false vacuum energy gets converted to the kinetic energy of the bubble wall) that bubble wall thickness decreases much faster (due to Lorentz contraction) compared to the bubble radius, as bubble collapse proceeds. Of course, eventually this type of *classical* evolution of bubble must stop, at least by the stage when the net size of the system has become smaller than that allowed by the uncertainty relation. The net energy E_f we start with (of the false vacuum bubble at the initial stage when free collapse of the interface commences), is much larger than a TeV. Thus, when collapsing bubble size becomes smaller than E_f^{-1} (say a TeV^{-1}), it seems reasonable that bubble collapse may halt. Entire energy E_f of the initial pure false vacuum bubble, which was subsequently converted into the kinetic energy of ultra-relativistic walls, may thus get converted to particles in a region of size less than $(E_f)^{-1}$. (It will be interesting to work out the exact conditions when bubble collapse will halt. Even if the bubble radius shrinks only to a value of say 0.1 fm, one still gets a hot spot, though with a lower temperature. It is also possible that in some situations, bubble collapse may develop strong anisotropies. In that case the bubble may break into smaller bubbles.)

It is important to realize that the above picture only requires that most, or a significant fraction, of the bubble wall energy (after bubble has collapsed to size of order 1 fm) is not dissipated away subsequently until different portions of the (Lorentz contracted) bubble wall collide with each other. This is because essentially all of the energy of the initial false vacuum bubble is already stored in the bubble walls by the time its radius shrinks to a value of order 1 fm (for initial radius much larger than 1 fm). Even with quantum fluctuations on the bubble wall background, there is no reason to expect that these fluctuations will tend to put an early stop on (or significantly dissipate the kinetic energy of) the highly relativistic bubble wall. For example, even for the case of nucleus-nucleus collision, interactions of wee partons do not stop the nuclei from overlapping (or going through) at sufficiently large collision energies. Though, we again emphasize that a nucleus, filled with partons, is a very different object than a *pure false vacuum bubble*. Thus, the arguments based on wee partons made for nucleus [34] do not extend in a natural way to the Lorentz contracted bubble wall. After all, one does not even know what is the correct field describing such a wall (apart from various possible order parameters), let alone the detailed nature of quantum fluctuations above the bubble wall separating deconfined and confined vacua of QCD (at zero temperature) and their Lorentz transformation properties. From all this, we would like to conclude that there seems a genuine possibility that bubble collapse may continue, preserving most of its energy, down to sizes much smaller than 1 fm. As we will see below, this possibility leads to very interesting implications.

The final conclusion is that the entire energy E_f of the false vacuum bubble will be

converted to a dense system of partons, contained in an extremely tiny region which can be as small as few TeV^{-1} to begin with (or even smaller). The energy of this bubble, E_f , is a fraction of the total energy of the initial parton system E_{tot} as given in Eq.(4). For $A = 200$, and with $\Delta z_i = 1$ fm, this fraction ranges from 15% to 40% for $\sqrt{s} = 5.5$ TeV, and 20% to 50% for $\sqrt{s} = 30$ TeV, as $B^{1/4}$ is decreased from 240 MeV to 120 MeV. For $\Delta z_i = 0.15$ fm, these fractions range from 5% to 20%, and 10% to 35% for the two values of \sqrt{s} respectively. For RHIC, with $\sqrt{s} = 200$ GeV, and with $\Delta z_i = 1$ fm, this fraction ranges from about 5% to 25%, as $B^{1/4}$ is decreased from 220 MeV to 100 MeV. We mention that here, as well as in later sections, for LHC, we will be considering a range of values of \sqrt{s} , including very large values such as 30 TeV (for Pb-Pb collision). This is with the idea that any possibility of observing new physics at such large energies, should provide strong motivation for going for such large (or even larger) values of \sqrt{s} .

V. EQUILIBRATION OF DECAY PRODUCTS OF BUBBLE WALL

Most of the energy of the initial parton system escapes out in the form of hadrons, and as we have seen above, only a fraction is left behind in the form of the vacuum energy inside the bubble. However, the important thing is that all this energy gets focused into a very tiny region due to ultra-relativistic collapse of the bubble wall. The resulting energy density can be extremely high. This parton system will then expand and in that process thermalize. For consistency of thermodynamic equilibrium, we must have a region of size at least of the order of the mean free path r_{eq} of the relevant degrees of freedom. For the relevant values of r_{eq} and the temperature, we find that due to small size of the hot spot, only strongly interacting particles can be in equilibrium. In naive perturbation theory, one would use interaction rate $\Gamma \sim \alpha_s^2 T$. With the value of $r_{eq} \sim (\alpha_s^2 T)^{-1}$, the resulting temperatures of the hot spot are rather low. However, as has been discussed in the literature [38,39], for QCD at finite temperature, there are serious problems such as infrared divergence and gauge dependence of results. An improved perturbation theory has been introduced by Braaten and Pisarski [38]. In this hard thermal loop re-summation technique, the relevant scattering cross-section rates are given as $\sim \alpha_s T$ for quark-quark scattering and $\sim 2\alpha_s T$ for gluon-gluon scattering [39]. With these results in view [39], we will estimate the resulting temperature T of the hot spot when its size is equal to,

$$r_{eq} \simeq (2.2\alpha_s T)^{-1} \quad (10)$$

and,

$$r_{eq} \simeq (\alpha_s T)^{-1} \quad (11)$$

First value of r_{eq} corresponds to the large interaction rate of gluons (say, for pure gluonic case [39]) and is relevant when only gluons equilibrate (size of the region being too small for quarks to effectively scatter). The second case (Eq.(11)) corresponds to the equilibration of the combined quark-gluon system.

Note, however, that the dynamics of equilibration of a rapidly evolving parton system is not too well understood. For example, estimates for equilibration time of partons at LHC

show [40] that the parton distributions approach equilibrium distributions within a duration of about 0.15 fm/c (with resulting QGP temperature being about 1 GeV). This time scale is too short compared to either of the estimates of r_{eq} given above. Even for g-g scattering the scattering rate given above will imply a time scale of about 0.5 fm (with $\alpha_s \sim 0.2$ for $T \sim 1$ GeV), for q-q scattering one should have expected a time scale of about 1 fm/c. Similarly, for RHIC, the estimated equilibration time [40] of 0.22 fm/c (with resulting QGP temperature of about 500 MeV) is still shorter than what one will get from above estimates of scattering rates. Keeping this in mind, we will also allow for the possibility that the decay products of bubble wall may also thermalize within a shorter time duration which we take to be 0.15 fm/c (this should be reasonable for hot spot temperature of about 1 GeV). Thus, along with the values of r_{eq} as given above by Eq.(10)-(11), we also consider the following value.

$$r_{eq} \simeq 0.15 \text{ fm} \quad (12)$$

It is clear that the use of constant r_{eq} can only be hoped to be a reasonable approximation over a limited temperature range. One may trust this value when temperature of the hot spot is obtained to be in the range of a couple of GeV.

An important point to note here is that in general the decay products of the bubble wall can include other particles as well, e.g. leptons, Higgs bosons etc. However, the electroweak coupling being much smaller, these degrees of freedom will take much longer to equilibrate, with effective temperature of the hot spot being very low (or, by that time the decay products may even freezeout). This means that only a fraction f of the total energy of the false vacuum bubble will be available in terms of quarks and gluons, remaining energy being carried by particles streaming out of the dense parton region. This is similar to the streaming out of direct photons and leptons from the early stages of parton production in relativistic heavy-ion collisions. Since the bubble wall separates the two phases of QCD, it is possible that its decay products will predominantly be quarks and gluons due to their larger cross-sections. Thus for estimating the maximum temperature of the equilibrated hot spot we will first assume that the entire energy of the false vacuum bubble goes in creating a thermal system of quarks and gluons.

With these arguments, the resulting temperature T_f of the hot spot at this stage can be determined by the following equation,

$$\frac{g_* \pi^2}{30} T_f^4 \frac{4\pi}{3} r_{eq}^3 + 4\pi r_{eq}^2 \sigma + \frac{4\pi}{3} r_{eq}^3 \rho = E_f \quad (13)$$

Here, $g_* = 37$ is the number of quark-gluon degrees of freedom. σ and ρ are the values of interface tension and false vacuum energy density as used earlier in Eq.(7) and Eq.(9). For the size of the region r_{eq} we will take various values as given by Eqs.(10)-(12). We use the following expression [41] for α_s as a function of temperature in Eqs.(10)-(11),

$$\alpha_s(T) = \frac{6\pi}{(33 - 2N_f) \ln(\frac{8T}{T_c})} \quad (14)$$

where T_c is the critical temperature, and we use number of flavors $N_f = 2$. With this expression for α_s , Eq.(13) is solved numerically to get T_f self consistently.

Note that when taking r_{eq} from Eq.(10), we are assuming that due to larger interaction rate, only gluons may thermalize, with quarks remaining out of equilibrium (within the region of size r_{eq}). In such a case g_* should be changed from 37 to 16, while at the same time E_f in the right hand side of Eq.(13) should be reduced by a factor $\frac{16}{37}$ (assuming equipartition of energy) as only this fraction of total bubble energy will thermalize. It turns out that this modification does not affect any results, the two factors effectively compensating for each other (i.e. other terms in Eq.(13) remain subdominant). We will thus not worry about this modification of the above equation and will continue to use Eq.(13) for all values of r_{eq} from Eqs.(10)-(12).

VI. RESULTS

We have obtained the value of T_f for a range of values of bag constant B , and for different values of A and initial energy density ϵ_i (which can be related to \sqrt{s} using Eq(1)). The value of surface tension of the wall σ is taken to be $64 \text{ MeV}/fm^2$ (for Eqs.(7),(9)), as determined using Eq.(6). We find that our results are rather insensitive to the value of σ . Changing σ to $1 \text{ MeV}/fm^3$ leads to virtually no change in T_f and r_f . Note that this means that our quantitative results may be valid even if the barrier height between the deconfining and confining vacua is very small, as long as shell structure can be justified. Increasing σ to even unreasonably large value of $300 \text{ MeV}/fm^3$ increases T_f by about 6 %, and decreases r_f by about 10 %.

A. LHC

Here, we present results for energies suitable for LHC. First we consider the case when only gluons equilibrate, so $r_{eq} = 2.2\alpha_s T$ (Eq.(10)). The physics here will be similar to the *two stage* model discussed in ref. [42] where gluons first thermalize to give higher temperature of the plasma, while quark equilibration takes a longer time resulting in lower temperature of the combined system. Here also we see that the largest values of T_f are obtained for this case. In Fig.4 we have plotted T_f (in GeV) vs. $B^{1/4}$ (in MeV) for the case when Δz_i (in Eq.(4)) is 1 fm. To give an idea how T_f varies with A , we give plots for three different values of A . Solid, dotted, and dashed curves correspond to $A = 200, 100,$ and 50 respectively. For subsequent figures, we will give plots only for the case $A = 200$. In Fig.4, plots have been given for $\sqrt{s} = 30, 15, 5.5 \text{ TeV}$, which can be translated to the values of $\epsilon_i \simeq 4.9, 2.8, 1.3 \text{ TeV}/fm^3$, respectively (for $A = 200$). Fig.4 also shows plots of the radius r_f of largest pure false vacuum bubble for $\sqrt{s} = 5.5 \text{ TeV}$. Note, the shell thickness Δr for these cases is of order $2R_A \simeq 13 \text{ fm}$.

Values of T_f are large in Fig.4 due to large interaction rate of gluons leading to rapid thermalization. This will be the highest temperature of an equilibrated system which can be expected in our model. Subsequently, quarks will also thermalize and the appropriate value of r_{eq} will be given by Eq.(11). The resulting values of T_f for the combined quark-gluon system are smaller as shown by the dotted plots in Fig.5. In this figure we also show plots (shown by dashed curves) for the case when r_{eq} is taken to have a fixed value equal to 0.15 fm . As we mentioned earlier in Sec.V, parton cascade simulations suggest that various

particle distributions approach equilibrium distributions within a time duration which may be as short as 0.15 fm/c for LHC with the associated QGP temperature of about 1 GeV. This time scale is much shorter than what one gets from the interaction rate in Eq.(11). Even the gluonic interaction rate (Eq.(10)) gives a significantly longer time scale. Thus we show plots for $r_{eq} = 0.15$ fm to allow for this possibility. As we mentioned in Sec.V, using a fixed value of r_{eq} means that the plots are not going to be reliable for a wide range of the temperature T_f of the hot spot. However, for the values of T_f around few GeV the plots may lead to reasonable estimates.

Plots in Figs.4,5 are with value of $\Delta z_i = 1$ fm in Eq.(4). In Fig.6 we show plots for the case when $\Delta z_i = 0.15$ fm. Resulting temperatures are much smaller now. As can be clearly seen from these plots, the temperature of the hot spot can easily reach well above 1 GeV, which is the expected initial temperature of the QGP here. Such a hot spot can lead to clean signals. Even for a reasonably conservative set of parameters, $r_{eq} = 0.15$ fm, $\Delta z_i = 0.15$ fm, and for the values of $B^{1/4}$ consistent with the critical temperature of about 170 MeV, the value of T_f can easily reach around 3 GeV (for $A = 200$, and with $\sqrt{s} = 5.5$ TeV).

B. RHIC

For RHIC, with $\sqrt{s} = 200$ GeV, for Au-Au collision, we find that T_f is very small and rarely reaches above 1 GeV. In Fig.7 we give plots for two choices, $\Delta z_i = 1$ fm and $= 0.22$ fm. For $\Delta z_i = 1$ fm case, solid and dashed plots correspond to r_{eq} given by Eq.(10) and Eq.(12) respectively. No solution is found for the case when $r_{eq} = \alpha_s T$ (Eq.(11)) for reasonable values of $B^{1/4}$. For $\Delta z_i = 0.22$ fm, solutions for reasonable values of $B^{1/4}$ are found only for the case when $r_{eq} = 0.15$ fm, as shown by the dashed plot. (As the temperature reaches about a GeV for this case, $r_{eq} = 0.15$ fm, which is the expected equilibration time at LHC, may be appropriate to use here). $A = 200$ for all these plots.

We have repeated the entire analysis for the case when entropy is conserved during parton expansion. In this case values of T_f are much smaller. We quote some values here to give an idea of the typical range of values of T_f for this case for various parameter values (with $A = 200$). As the largest values of T_f are obtained for the case when only gluons equilibrate, we give here numbers for the case when $r_{eq} = 2.2\alpha_s T$. For $\sqrt{s} = 30$ TeV and with $\Delta z_i = 1$ fm, we get T_f varying from 6.2 GeV to about 5.3 GeV as $B^{1/4}$ increases from 100 MeV to 240 MeV. (The range of T_f becomes from 3.9 GeV to 3.3 GeV for $A = 100$.) For $\sqrt{s} = 15$ TeV, the corresponding values of T_f range from 4.2 GeV to about 3.5 GeV. For $\sqrt{s} = 5.5$ TeV, T_f ranges from 2.4 GeV to 2 GeV for the same range of $B^{1/4}$. For $\Delta z_i = 0.15$ fm, T_f is much smaller, ranging from 1.2 GeV to 0.8 GeV even with $\sqrt{s} = 30$ TeV. We mention again, as discussed above, due to non-equilibrium conditions, energy conserving expansion may be more appropriate in our case.

C. Possibility of non-thermal restoration of electroweak symmetry?

So far we have presented results estimating the temperature of the hot spot, assuming the equilibration of the decay products (or a fraction of them) resulting from the bubble wall. As the collapsing bubble concentrates a very large energy in a very tiny region, the

resulting initial parton system will be extremely dense. The decay of ultra-relativistic bubble walls should lead to rapid particle production. When wall energy is sufficiently high (say for LHC case) then decay products may also consist of a sizeable density of the Standard model Higgs particles among other decay products. This type of picture reminds one of the rapid particle production at the end of inflationary phase in the early Universe where the inflaton field decays into particles. A very interesting possibility which has been proposed in that context [4] is that, during the early stages of particle production, even when the system remains in a non-equilibrium state, one may still get restoration of symmetry due to modification of the effective potential from large population of particle modes resulting from the decay of the inflaton.

This raises the question whether a similar phenomenon can also occur within the context of our model. The decay of ultra-relativistic bubble walls will lead to rapid population of various particle modes (including the scalar particles). It may then be possible for the *electroweak* effective potential to be modified, leading to effective restoration of electroweak symmetry, even if the whole system remains in a non-equilibrium state. In fact, even for the early evolution of the quark-gluon system resulting from collision of the two nuclei, one may be able to study this possibility and see if, for example, chiral symmetry may get restored at a very early stage when the whole parton system is still in a non-equilibrium state. We hope to check both these possibilities more carefully in future. For our present purpose, we will simply assume that such a non-thermal restoration of electroweak symmetry can indeed happen, and present the estimates corresponding to such a scenario.

It is fair to say that at this stage this remains a speculation. Thus the results of this subsection should only be taken as representing many new interesting possibilities which may open up in the context of our model. The reason that we are considering this speculation is that it may imply the possibility of experimental investigation of the baryon number violation in these experiments.

In the absence of a more complete treatment of the non-equilibrium problem at hand, we will continue to use language of equilibrium system to discuss even this possibility. Thus, from the resulting energy densities, we will estimate an effective temperature T_{eff} . This effective temperature, in the context of non-thermal symmetry restoration, will only represent whether the symmetry restoration can happen, and if it does happen, how far the system is into the symmetric phase, away from the transition point. Clearly all these numbers are to be taken as only giving a crude picture of the possibility of symmetry restoration.

In the absence of thermal equilibrium one needs some other estimate for the size of the region. As we have mentioned, we will translate the energy densities to an effective temperature T_{eff} (which should be taken as giving a scale representing the properties of the effective potential). It may not be an unreasonable guess then to take the system size also to be given by the same scale, i.e. T_{eff}^{-1} . Since our motivation is only to see if the densities are large enough at least to be consistent with the restoration of electroweak symmetry, we will take the size of the region to be given simply by T_{ew}^{-1} , where $T_{ew} \simeq 100$ GeV is the transition temperature for the electroweak symmetry breaking. With this, we will again estimate the temperature T_f (which we now denote as T_{eff} since it should be taken as a parameter characterizing the modification of the effective potential) of the dense spot using Eq.(13), but now with $r_{eq} = T_{ew}^{-1}$.

However, as we will see, in the case of LHC energies one gets $T_{eff} > T_{ew}$ which we interpret as the possibility of electroweak symmetry restoration. For such a situation, we also include electroweak degrees of freedom in Eq.(13), i.e. we take $g_* = 100$. Also, we use the QCD values for the values of interface tension σ and false vacuum energy density ρ in Eq.(13) when T_{eff} comes out to be less than 100 GeV, and use the values (again, only in Eq.(13)) typical of the electroweak scale, i.e., $\sigma \simeq T_{ew}^3$, and $\rho \simeq T_{ew}^4$, when the T_{eff} exceeds 100 GeV. There is a technical problem in solving for T_{eff} in this manner from Eq.(13). When T_{eff} is exactly equal to 100 GeV, then one must allow for the changeover in the value of ρ from the value relevant to QCD to the value relevant for the electroweak symmetric vacuum (i.e., the latent heat of the electroweak phase transition). We take care of this by using the following prescription. Below, we will be giving plots of T_{eff} as a function of $B^{1/4}$. As the value of $B^{1/4}$ is decreased, it corresponds to increasing value of E_f , and consecutively, increasing value of T_{eff} (via Eq.(13)). For some cases, as $B^{1/4}$ is decreased, T_{eff} increases from a value below 100 GeV, and we reach a point when T_{eff} just equals 100 GeV (for the size of the region equal to $(100 \text{ GeV})^{-1}$). For these values of $B^{1/4}$, we use QCD values for ρ' and σ' . As $B^{1/4}$ is decreased further, E_f increases, but this increase is not enough to convert entire region of size $(100 \text{ GeV})^{-1}$ into the electroweak symmetric phase (i.e., appropriate for using electroweak values of ρ' and σ'). However, a region of somewhat smaller size can always be in the electroweak symmetric phase. Equivalently, the region of size $(100 \text{ GeV})^{-1}$ will be in the mixed phase. The temperature T_{eff} will remain fixed equal to 100 GeV for these values of $B^{1/4}$. Eventually a value of $B^{1/4}$ will be reached which leads to large enough E_f which can convert the whole region of size $(100 \text{ GeV})^{-1}$ into the electroweak symmetric phase. Thus, in the plots below, when T_{eff} crosses the value 100 GeV, there will be a very small range of $B^{1/4}$ for which T_{eff} will remain constant, equal to 100 GeV.

As we discuss this possibility motivated by the non-thermal restoration of the electroweak symmetry, we will not present results for the case of RHIC as there we find T_{eff} to be always much less than 100 GeV. Since T_{eff} should not be interpreted as the temperature of the hot spot, it is not clear what implications one can obtain from this value of T_{eff} for RHIC.

Fig.8 gives plots of T_{eff} for different parameters for the case $\Delta z_i = 1$. We see that for $A = 200$, T_{eff} is well above $T_{ew} \simeq 100 \text{ GeV}$ (with $\Delta z_i = 1 \text{ fm}$) even for $\epsilon_i \simeq 1.3 \text{ TeV/fm}^3$ which is roughly the expected energy density at the initial stage in Pb-Pb collision at $\sqrt{s} = 5.5 \text{ TeV}$ at LHC. Such a large value of T_{eff} indicates extremely dense particle system, which may be taken as indicating a strong possibility of non-thermal restoration of electroweak symmetry. Interesting thing is that even for rather small values of $A = 50$, it is possible to get $T_{eff} > T_{ew}$ by using large values of \sqrt{s} . This is important since early freezeout is more natural for small values of A . Fig.9 shows similar plots for the case when Δz_i in Eq.(4) is equal to 0.15 fm. Resulting values of T_{eff} are much smaller now, and for $\sqrt{s} = 5.5 \text{ TeV}$ resulting T_{eff} is smaller than $T_{ew} \sim 100 \text{ GeV}$.

VII. DISCUSSION AND CONCLUSIONS

The possibility of producing a false vacuum bubble in laboratory in the context of relativistic quantum field theory will have important implications. Bubble wall propagation, its collapse and eventual decay into particles are issues which have relevance for various phase

transitions in the early universe. As we have argued, such a false vacuum bubble should lead to a hot spot with temperature which may be well in excess of the initial temperature of the QGP system (as given by the initial energy density ϵ_i). For example, even for a reasonably conservative set of parameters, the temperature of the hot spot can reach as high as 3 GeV for LHC (as shown by the dashed plot in Fig.6 for $\sqrt{s} = 5.5$ TeV case). One may get much higher temperatures for more optimistic values of various parameters. Such a hot spot will have many obvious signals. For example, one will expect increased production of heavy quarks. There should be anomalous production of very large P_T partons, dileptons, and photons (depending on what is the distribution of the decay product from the decay of colliding bubble walls). Of course if the bubble collapse does not proceed to sizes much smaller than 1 fm (for example, due to quantum fluctuations on the bubble wall background, or if the center of the shell is not entirely devoid of partons, or if the bubble breaks up due to asphericity before collapsing to very small sizes), the resulting temperature for this 1 fm size hot spot may not be large enough to lead to clean signals.

We have also speculated on the possibility that due to dense parton system resulting from the decay of bubble walls, one may get non-thermal restoration of electroweak symmetry. If that happens then it may open up the possibility of observing unsuppressed baryon number violation via sphaleron processes [6,7,8]. An important issue in this regard is the size of the region as compared to the sphaleron size. Below T_{ew} , when electroweak symmetry is broken, sphaleron is a solution of classical equations of motion. Baryon number violating processes are dominated by sphalerons [7] with a size of order $(3 \text{ GeV})^{-1}$. This is a very large region compared to the size we have considered above, i.e. $(100 \text{ GeV})^{-1}$. If we consider the size of the hot spot to be about $(3 \text{ GeV})^{-1}$, then resulting values of T_{eff} never exceed about 15 GeV. It is not clear what really should be the lower limit for the size of the region for sphaleron interactions to occur in the symmetric phase [7,8]. It is possible that in the symmetric phase, sphaleron processes in smaller regions may not be too suppressed [7]. Even in the symmetry broken phase, the core of sphaleron is only about $(20 \text{ GeV})^{-1}$ large [8]. For hot spot of size $\sim (20 \text{ GeV})^{-1}$, we find that T_{eff} is less than about 65 GeV, even with $A = 200$, and $\sqrt{s} = 30$ TeV (with $\Delta z_i = 1$ fm).

In conclusion, we have discussed the possibility that under certain situations, when a shell like expanding parton system emerges from the collision of ultra-relativistic nuclei, a bubble of pure false vacuum may be left behind. We find that the net energy of this bubble may be a significant fraction of the total energy of the initial parton system. This bubble undergoes free, relativistic collapse. Due to extremely large Lorentz contraction factor, the bubble wall thickness decreases faster than the bubble radius. Due to this, bubble contraction proceeds down to very small scales, much smaller than the typical QCD scale of 1 fm (assuming that any quantum fluctuations on the background of the collapsing ultra-relativistic wall do not dissipate most of its energy when bubble radius is about 1 fm). Eventually different portions of bubble wall collide, converting all of their kinetic energy (which equals the initial bubble energy) into particles. These particles may eventually thermalize, leading to a hot spot. We have estimated the expected temperatures in this hot spot and find that it can be well above the initial temperature of the QGP system. There will be clear signals of such hot spots, such as increased production of heavy quarks, very large P_T partons, dileptons, photons etc.

ACKNOWLEDGEMENTS

We are very thankful to Pankaj Agrawal, Sanatan Digal, Avijit Ganguly, Amit Kundu, Biswanath Layek, Shashi Phatak, and Supratim Sengupta for useful discussions and comments.

REFERENCES

- [1] U. Heinz, Nucl. Phys. **A685** (2001) 414 ; N.V.Eijndhoven, hep-ph/0012149.
- [2] For a recent review, see J.L.Nagle and T.S. Ullrich, nucl-ex/0203007.
- [3] M.A. Stephanov, Nucl. Phys. **A661** (1999) 403; M. Stephanov, K. Rajagopal, and E. Shuryak, Phys. Rev. Lett. **81** (1998) 4816; M. Alford, K. Rajagopal, and F. Wilczek, Phys. Lett. **B422** (1998) 247.
- [4] L. Kofman, A. Linde, and A.A. Starobinsky, Phys. Rev. Lett. **76** (1996) 1011; S. Khlebnikov, L. Kofman, A. Linde, and I. Tkachev, Phys. Rev. Lett. **81** (1998) 2012; I. Tkachev, S. Khlebnikov, L. Kofman, and A. Linde, Phys. Lett. **B440** (1998) 262; M.F. Parry and A.T. Sornborger, Phys. Rev. **D60** (1999) 103504.
- [5] A. Ringwald, Nucl. Phys. **B330** (1990) 1; L. McLerran, A. Vainshtein, and M. Voloshin, Phys. Rev. **D42** (1990) 180; V.V. Khoze and A. Ringwald, Nucl. Phys. **B355** (1991) 351; D.I. Diakonov and V. Yu Petrov, Phys. Lett. **B275** (1992) 459; M.J. Gibbs, A. Ringwald, B.R. Webber, and J.T. Zadrozny, Z. Phys. **C66** (1995) 285; See also, V.A. Rubakov and M.E. Shaposhnikov, Phys. Usp. **39** (1996) 461, and references therein.
- [6] For reviews see, A.G. Cohen, D.B. Kaplan and A.E. Nelson, Annu. Rev. Nucl. Part. Sci. **43** (1993) 27; M. Trodden, Rev. Mod. Phys. **71** (1999) 1463.
- [7] P. Arnold and L. McLerran, Phys. Rev. **D36** (1987) 581; O. Philipsen, Phys. Lett. **B358** (1995) 210.
- [8] F.R. Klinkhamer and N.S. Manton, Phys. Rev. **D30** (1984) 2212.
- [9] C. Greiner and D.H. Rischke, Phys. Rev. **C54** (1996) 1360; A. Abada and J. Aichelin, Phys. Rev. Lett. **74** (1995) 3130;
- [10] D. Teaney and E.V. Shuryak, Phys. Rev. Lett. **83** (1999) 4951.
- [11] J.D. Bjorken, K.L. Kowalski and C.C. Taylor, in *Results and Perspectives in Particle Physics 1993*; Proceedings of the 7th Rencontres de Physique de la Vallée d'Aoste, La Thuile, Italy, 1993, edited by M. Greco (Editions Frontieres, Gif-sur-Yvette, France, 1993); G. Amelino-Camelia, J.D. Bjorken, and S.E. Larsson, Phys. Rev. **D56** (1997) 6942;
- [12] I.N. Mishustin and O. Scavenius, Phys. Rev. Lett. **83** (1999) 3134.
- [13] S.A. Bass and A. Dumitru, Phys. Rev. **C61** (2000) 064909; A. Dumitru, Phys. Lett. **B463** (1999) 138.
- [14] T. Csorgo and L.P. Csernai, Phys. Lett. **B333** (1994) 494; J.P. Bondorf, H. Feldmeier, I.N. Mishustin, and G. Neergaard, Phys. Rev. **C65** (2002) 017601.
- [15] K.J. Eskola, K. Kajantie, P.V. Ruuskanen, and K. Tuominen, Nucl. Phys. **B570** (2000) 379.
- [16] K.J. Eskola, P.V. Ruuskanen, S.S. Rasanen, and K. Tuominen, hep-ph/0104010.
- [17] A. Krasnitz and R. Venugopalan, Phys. Rev. Lett. **84** (2000) 4309; N. Hammon, H. Stocker, and W. Greiner, Phys. Rev. **C61** (2000) 014901.
- [18] J.D. Bjorken, Phys. Rev. **D27** (1983) 140.
- [19] L.P. Csernai and I.N. Mishustin, Phys. Rev. Lett. **74** (1995) 5005.
- [20] S. Digal and A.M. Srivastava, Phys. Rev. Lett. **80** (1998) 1841.
- [21] L.D. McLerran and B. Svetitsky, Phys. Rev. **D24** (1981) 450; B. Svetitsky, Phys. Rept. **132** (1986) 1.
- [22] For reviews, see, A. Albrecht, astro-ph/0007247; K.A. Olive, Phys. Rept. **190** (1990) 307.
- [23] N. Borghini, W.N. Cottingham, and R. V. Mau, J.Phys. **G26** (2000) 771.

- [24] R.D. Pisarski, Phys. Rev. **D62** (2000) 111501; *ibid*, hep-ph/0101168.
- [25] S.C. Phatak, Phys. Rev. **C58** (1998) 2383.
- [26] H.B. Nielsen and A. Patkos, Nucl. Phys. **B195** (1982) 137; L.R. Dodd, A.G. Williams, and A.W. Thomas, Phys. Rev. **D35** (1987) 1040; A. Drago, M. Fiolhais, and U. Tambini, Nucl. Phys. **A588** (1995) 801; A. Mazzolo, J.-F. Mathiot, and R.M. Galain, Phys. Lett. **B274** (1992) 154.
- [27] J. Ignatius, K. Kajantie, H. Kurki-Suonio, and M. Laine, Phys. Rev. **D49** (1994) 3854.
- [28] L.P. Csernai and J.I. Kapusta, Phys. Rev. **D46** (1992) 1379.
- [29] J.C. Miller and O. Pantano, Phys. Rev. D **40** (1989) 1789; **42** (1990) 3334.
- [30] M.B. Voloshin, I.Yu. Kobzarev and L.B. Okun, Yad. Fiz. **20** (1974) 1229 [Sov. J. Nucl. Phys. **20** (1975) 644]; S. Coleman, Phys. Rev. **D15** (1977) 2929.
- [31] A.M. Srivastava, Phys. Rev. **D45** (1992) R3304.
- [32] E. Witten, Phys. Rev. D **30** (1984) 272; S.A. Bonometto and O. Pantano, Phys. Rep. **228** (1993) 175.
- [33] P. Danielewicz and M. Gyulassy, Phys. Rev. **D31** (1985) 53.
- [34] R. Venugopalan, Nucl. Phys. **A590** (1995) 147c.
- [35] L. Susskind, Phys. Rev. **D49** (1994) 6606.
- [36] L.M. Widrow, Phys. Rev. **D40** (1989) 1002.
- [37] D.W. Neilsen and M.W. Choptuik, Class. Quant. Grav. **17** (2000) 733.
- [38] E. Braaten and R.D. Pisarski, Nucl. Phys. **B337** (1990) 569.
- [39] M.H. Thoma, Phys. Rev. **D49** (1994) 451.
- [40] K. Geiger, Phys. Rept. **258** (1995) 237.
- [41] S.-Y. Wang, D. Boyanovsky, and K.-W. Ng, Nucl. Phys. **A699** (2002) 819.
- [42] E. Shuryak, Phys. Rev. Lett. **68** (1992) 3270.

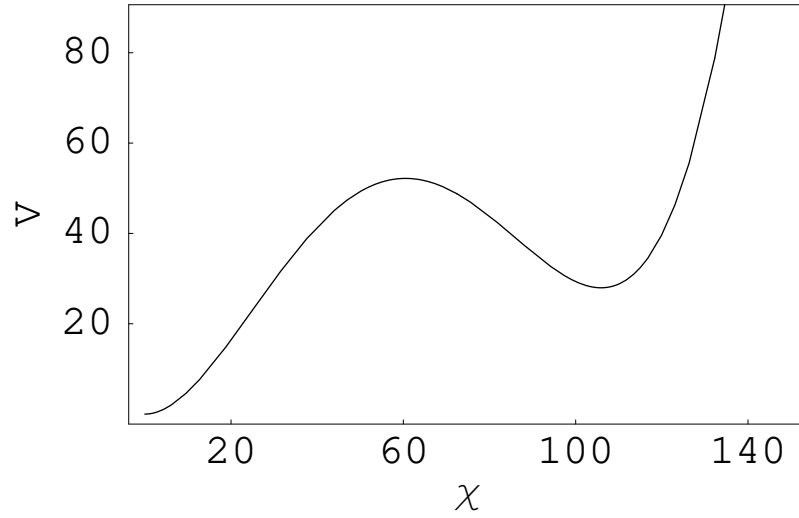


FIG. 1.

Plot of $V(\chi)$ (in MeV/fm³) vs. χ (in MeV), as given in Eq.(3). The absolute minimum at $\chi = 0$ corresponds to the confining true vacuum while the local minimum at $\chi \neq 0$ corresponds to the metastable deconfining vacuum.

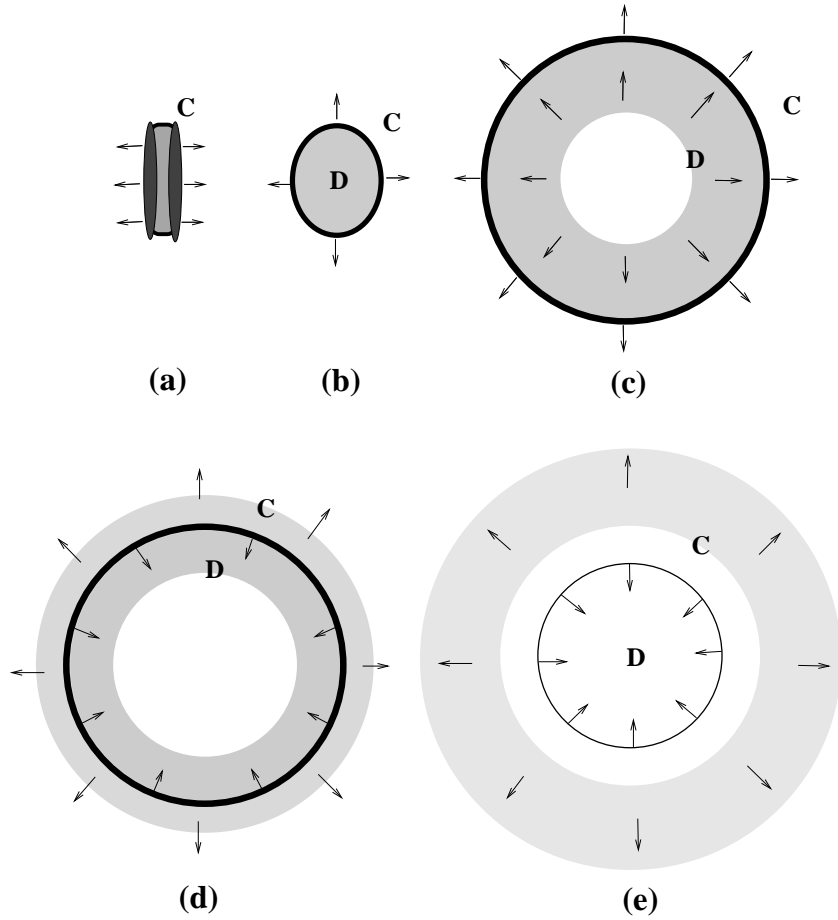


FIG. 2.

(a) The initial stage showing beginning of longitudinal expansion of the parton system between the two nuclei receding after overlap. (b) Beginning of transverse expansion. C and D denote regions with confining vacuum and deconfining vacuum, respectively. Thick solid line at the boundary denotes the interface separating the two vacua. (c) Development of shell structure with depletion of partons in the center due to expansion. (d) Stage of hadronization of the parton shell as the interface shrinks through the shell. (e) Relativistic collapse of the interface. Interface is shown to be thinner due to Lorentz contraction.

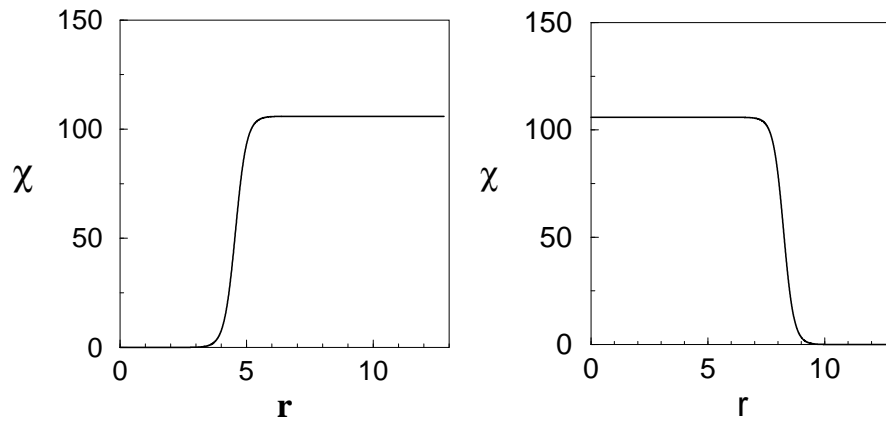


FIG. 3.

Left figure shows the true vacuum quantum bubble obtained as the solution of Eq.(5). Right figure shows the false vacuum bubble obtained by inverting the profile of the true vacuum bubble. χ is in MeV and r is in fm.

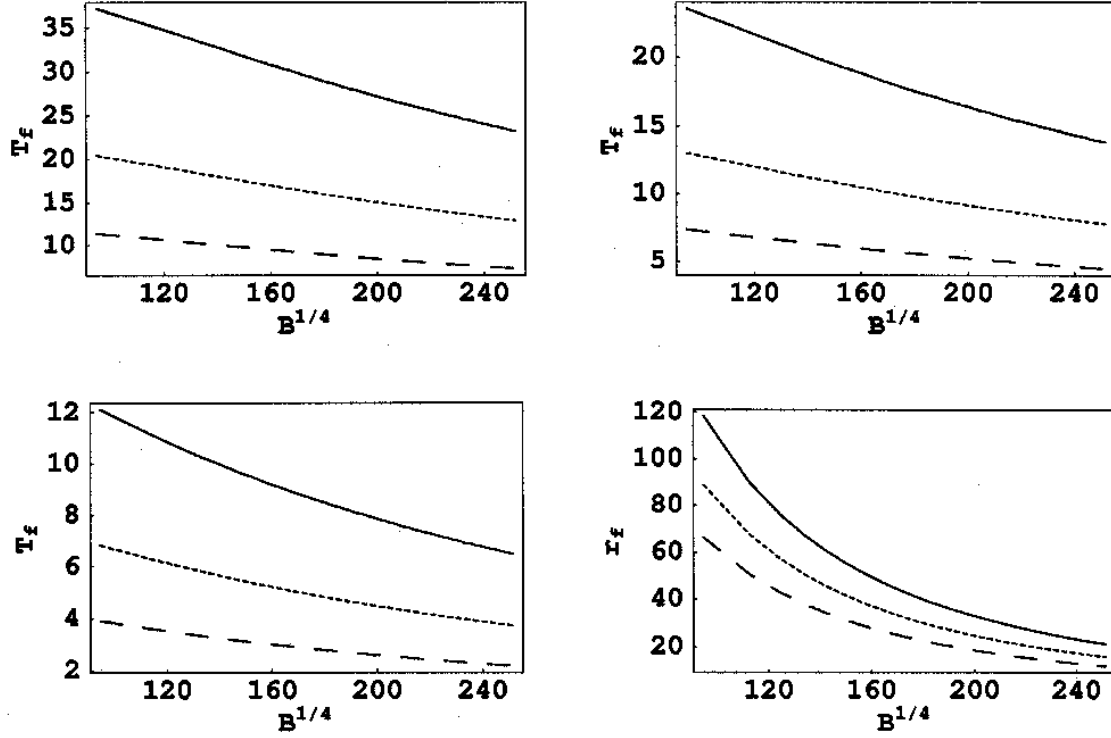


FIG. 4.

Figures on top left and top right correspond to $\sqrt{s} = 30$ and 15 TeV, respectively. Bottom two figures correspond to $\sqrt{s} = 5.5$ TeV. T_f is in GeV, $B^{1/4}$ in MeV, and r_f is in fm. Solid, dotted, and dashed curves correspond to $A = 200, 100,$ and 50 respectively. These plots correspond to $\Delta z_i = 1$ fm in Eq.(4). These plots are for r_{eq} given in Eq.(10) corresponding to the case when only gluons thermalize.

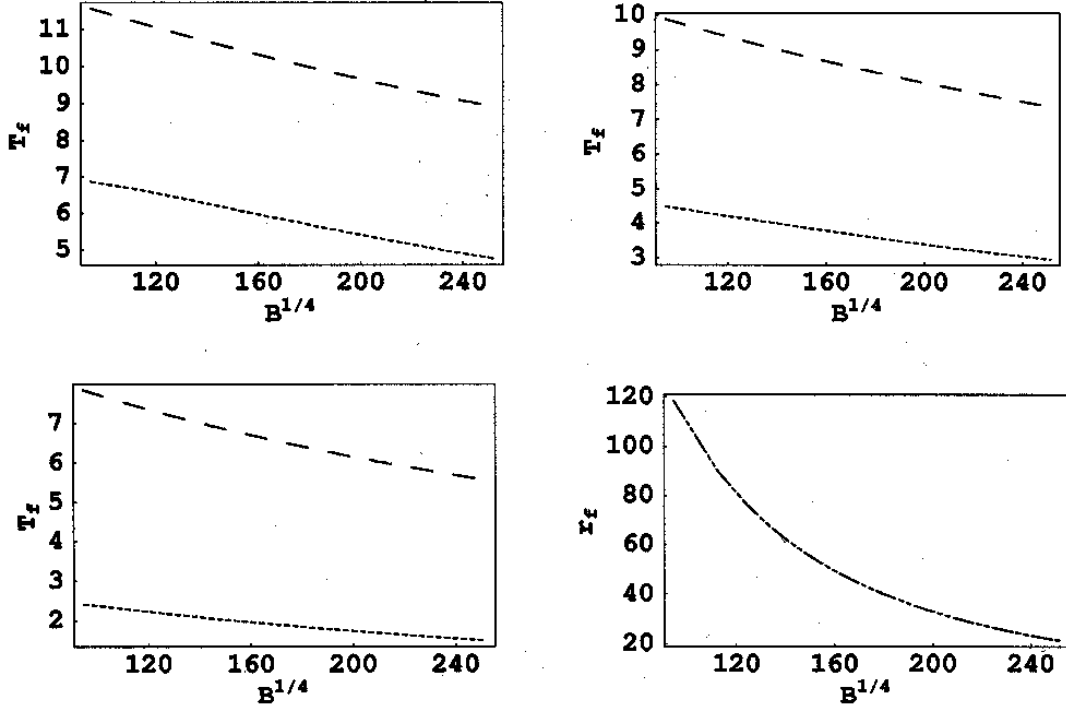


FIG. 5.

All plots in this figure correspond to $A = 200$. Figures on top left and top right correspond to $\sqrt{s} = 30$ and 15 TeV, respectively. Bottom two figures correspond to $\sqrt{s} = 5.5$ TeV. T_f is in GeV, $B^{1/4}$ in MeV, and r_f is in fm. Dotted and dashed curves correspond to the two cases, $r_{eq} = \alpha_s T$ (Eq.(11)), and $r_{eq} = 0.15$ fm respectively. Plot of r_f shows bubble radius for both these cases. (It is the same as the plot of r_f shown by the solid curve in Fig.4.) These plots correspond to $\Delta z_i = 1$ fm in Eq.(4).

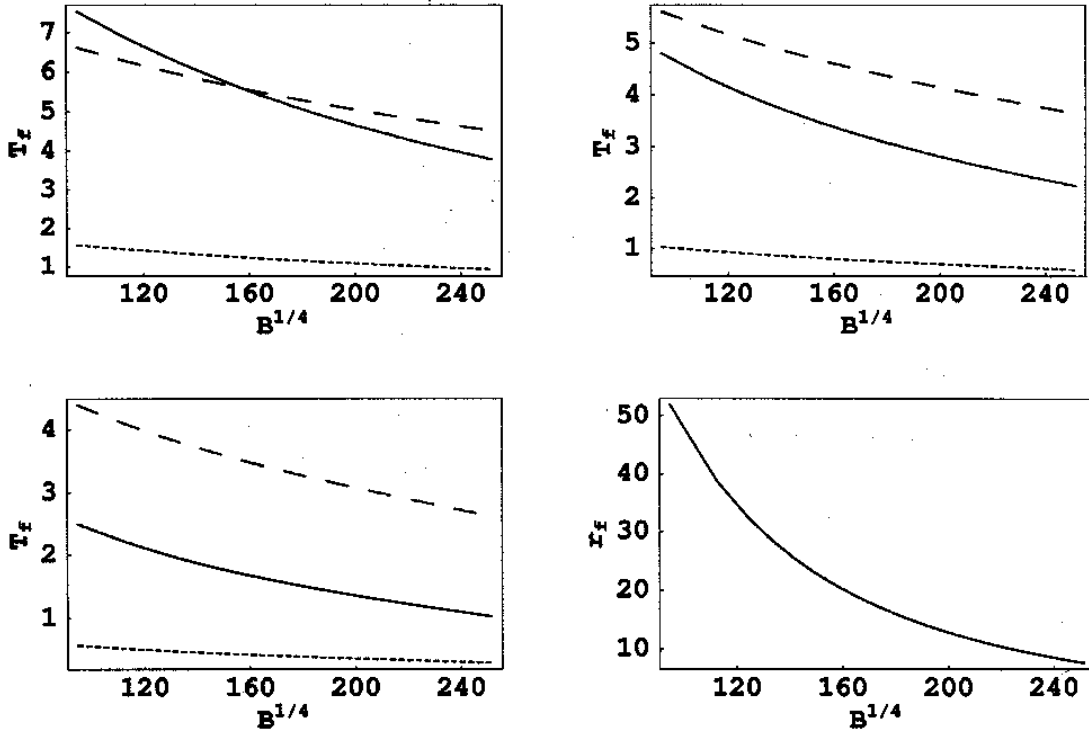


FIG. 6.

Similar plots as in Fig.5, but now with $\Delta z_i = 0.15$ fm. Here we show three plots in each figure for T_f . Solid, dotted, and dashed plots correspond to the three choices for r_{eq} as given by Eq.(10)-(12), respectively.

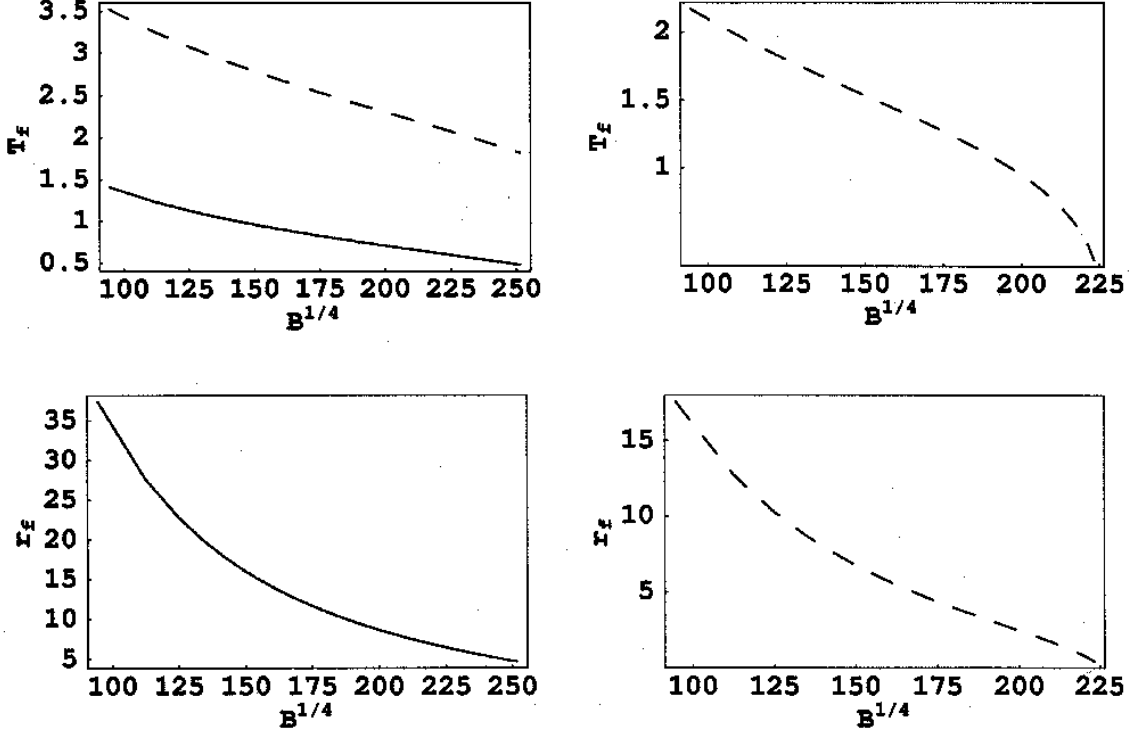


FIG. 7.

Plots for $\sqrt{s} = 200$ GeV. Figures on top left and top right correspond to Δz_i (in Eq.(4)) = 1 fm and 0.22 fm respectively. Figures below these give corresponding plots of the shell radius r_f . For $\Delta z_i = 1$ fm case, solid and dashed plots correspond to r_{eq} given by Eq.(10) and Eq.(12) respectively. No solution is found for the case when $r_{eq} = \alpha_s T$ (Eq.(11)) for reasonable values of $B^{1/4}$. For $\Delta z_i = 0.22$ fm, solutions for reasonable values of $B^{1/4}$ are found only for the case when $r_{eq} = 0.15$ fm, as shown by the dashed plot. $A = 200$ for all these plots.

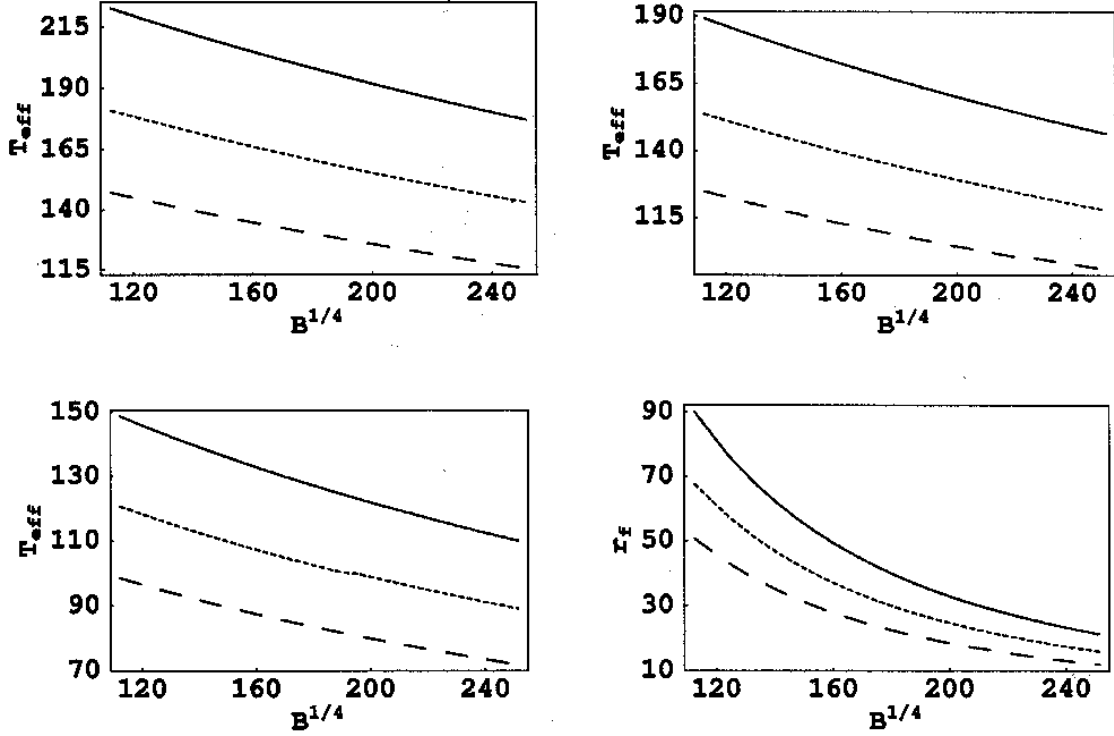


FIG. 8.

Figures on top left and top right correspond to $\sqrt{s} = 30$ and 15 TeV, respectively. Bottom two figures correspond to $\sqrt{s} = 5.5$ TeV. T_{eff} is in GeV, $B^{1/4}$ in MeV, and r_f is in fm. Solid, dotted, and dashed curves correspond to $A = 200, 100,$ and 50 respectively. These plots correspond to $\Delta z_i = 1$ fm in Eq.(4). (Note that the range of $B^{1/4}$ in the plots here and in Fig.9 is slightly different from the range in Figs.4-7.)

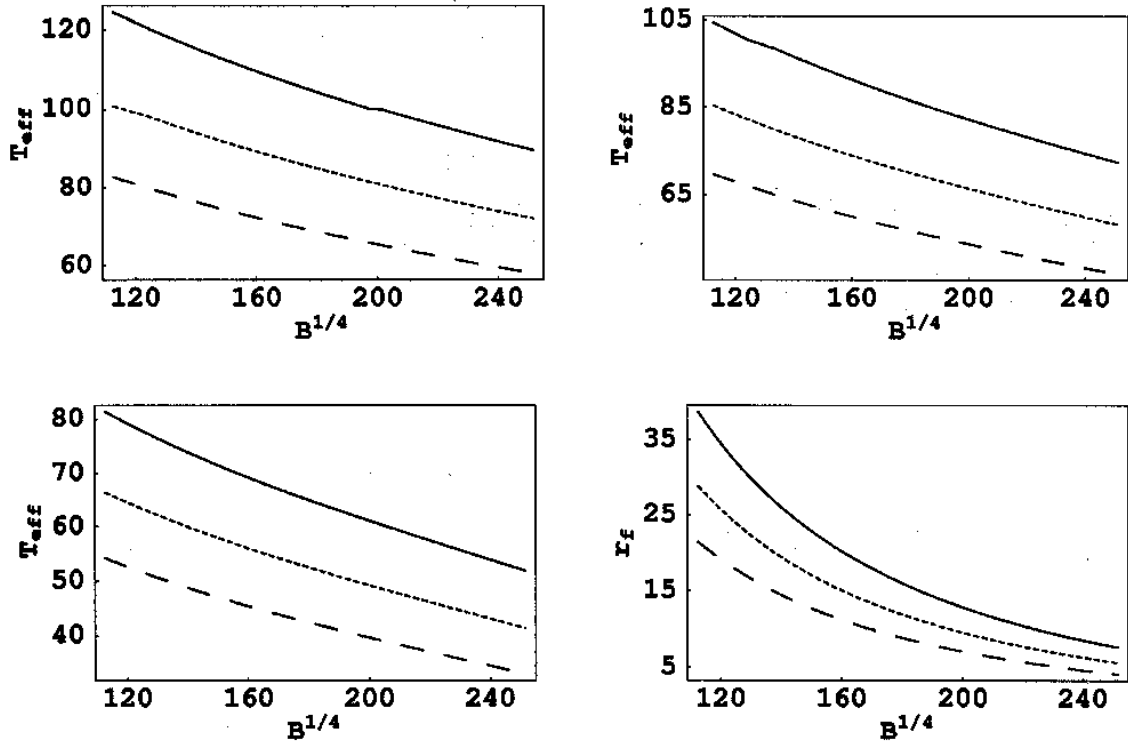


FIG. 9.

Same plots as in Fig.8, but with $\Delta z_i = 0.15$ fm in Eq.(4).